

Seco-Porphyrazines: Synthetic, Structural, and Spectroscopic Investigations

Antonio Garrido Montalban,[†] Steven J. Lange,[‡] L. Scott Beall,[†] Neelakandha S. Mani,[§] David J. Williams,[†] Andrew J. P. White,[†] Anthony G. M. Barrett,^{*,†} and Brian M. Hoffman^{*,‡}

Department of Chemistry, Imperial College of Science, Technology and Medicine, South Kensington, London SW7 2AY, U.K., Department of Chemistry, Northwestern University, Evanston, Illinois 60208, and Department of Chemistry, Colorado State University, Fort Collins, Colorado 80523

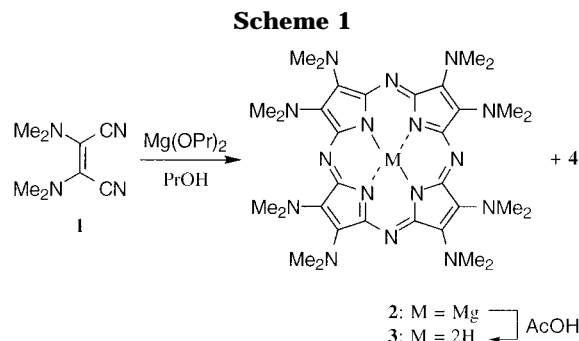
Received August 27, 1997[®]

Linstead macrocyclization of dinitrile **1** gave [octakis(dimethylamino)porphyrazinato]magnesium(II) **2** and the seco-porphyrazine **4** from adventitious oxidation. The structure of the latter has been unequivocally established by an X-ray crystallographic study. Alternatively, compound **4** was obtained in high yield from the manganese dioxide-mediated oxidation of the free base porphyrazine **3**. This convenient method was further extended to core metalated and unsymmetrical porphyrazines. In crystals of zinc–seco-porphyrazine **11**, the molecules exist as face-to-face dimers linked via complexation of the zinc center in one molecule to one of the amide oxygen atoms in the other and *vice versa*. The cleaved pyrrole ring in seco- and diseco-porphyrazines causes a ~50–70 nm red-shifted split Q-band in the electronic absorption spectra.

Introduction

Peripherally functionalized porphyrazines (tetraaza-porphyrins) and related macrocycles can bind multiple metal ions, have the potential to exhibit novel magnetic and electronic properties, and serve as building blocks in the assembly of higher order polymetallic arrays.¹ A range of different substituents provides porphyrazine ligands with interesting useful new features, including greatly enhanced organic solubility compared to their phthalocyanine counterparts. The preparation of symmetric octathio-porphyrazines has recently been described.^{2–4} Peripheral coordination of Sn(IV)^{2,3} or Ni(II)⁴ resulted in the isolation and crystallographic characterization of *star*-porphyrazines. In addition, we have recently reported the synthesis of related unsymmetrical *Gemini*-⁵ and *solitaire*-porphyrazines.⁶

We have also described the synthesis of the octakis-(dimethylamino)porphyrazine **2** (MgODMAPz)⁷ and derivatives of porphyrzinoctaoil,⁸ two ligands functionalized with nitrogen and oxygen atoms, respectively, in place of sulfur. The free base **3** (H₂ODMAPz) is more readily oxidized than ferrocene⁹ and forms charge-transfer complexes with tetracyanoquinodimethane



(TCNQ) and C₆₀.¹⁰ We observed that a minor side product, the seco-porphyrazine **4**, was formed during the Linstead macrocyclization of bis(dimethylamino)maleonitrile (**1**). Subsequently we found that acid-mediated demetalation of the magnesium porphyrazine **2** resulted in peripheral oxidation of one pyrrole ring to reveal the seco-porphyrazine **4**.¹¹ After our report, a related structural type (2,3-secochlorin-2,3-dione) has been described.¹² We speculated that this oxidative desymmetrization may have resulted via the formation of singlet oxygen. Herein we report full experimental data on the synthesis of MgODMAPz (**2**), further studies on ring oxidation, and the coordination chemistry of the derived macrocycles **6**, **7**, and **11**.

Results and Discussion

Commercial, inexpensive diaminomaleonitrile was readily converted into the tetramethyl derivative **1** following the method reported by Begland *et al.*¹³ Linstead¹⁴ macrocyclization of **1** using magnesium propoxide

[†] Imperial College.

[‡] Northwestern University.

[§] Colorado State University.

[®] Abstract published in *Advance ACS Abstracts*, December 1, 1997.

(1) *Phthalocyanines: Properties and Applications*, Leznoff, C. C., Lever, A. B. P., Ed.; VCH: Weinheim, 1989; Vols. 1 and 2.

(2) Velázquez, C. S.; Broderick, W. E.; Sabat, M.; Barrett, A. G. M.; Hoffman, B. M. *J. Am. Chem. Soc.* **1990**, *112*, 7408.

(3) Velázquez, C. S.; Fox, G. A.; Broderick, W. E.; Andersen, K. A.; Anderson, O. P.; Barrett, A. G. M.; Hoffman, B. M. *J. Am. Chem. Soc.* **1992**, *114*, 7416.

(4) Velázquez, C. S.; Baumann, T. F.; Olmstead, M. M.; Hope, H.; Barrett, A. G. M.; Hoffman, B. M. *J. Am. Chem. Soc.* **1993**, *115*, 9997.

(5) Sibert, J. W.; Baumann, T. F.; Williams, D. J.; White, A. J. P.; Barrett, A. G. M.; Hoffman, B. M. *J. Am. Chem. Soc.* **1996**, *118*, 10487.

(6) (a) Baumann, T. F.; Sibert, J. W.; Olmstead, M. M.; Barrett, A. G. M.; Hoffman, B. M. *J. Am. Chem. Soc.* **1994**, *116*, 2639. (b) Baumann, T. F.; Nasir, M. S.; Sibert, J. W.; White, A. J. P.; Olmstead, M. M.; Williams, D. J.; Barrett, A. G. M.; Hoffman, B. M. *J. Am. Chem. Soc.* **1996**, *118*, 10479.

(7) Mani, N. S.; Beall, L. S.; Miller, T.; Anderson, O. P.; Hope, H.; Parkin, S. R.; Williams, D. J.; Barrett, A. G. M.; Hoffman, B. M. *J. Chem. Soc., Chem. Commun.* **1994**, 2095.

(8) Cook, A. S.; Williams, D. B. G.; White, A. J. P.; Williams, D. J.; Lange, S. J.; Barrett, A. G. M.; Hoffman, B. M. *Angew. Chem., Int. Ed. Engl.* **1997**, *36*, 760.

(9) Goldberg, D. P.; Garrido Montalban, A.; White, A. J. P.; Williams, D. J.; Barrett, A. G. M.; Hoffman, B. M. Manuscript in preparation.

(10) Eichhorn, D. M.; Yang, S.; Jarrell, W.; Baumann, T. F.; Beall, L. S.; White, A. J. P.; Williams, D. J.; Barrett, A. G. M.; Hoffman, B. M. *J. Chem. Soc., Chem. Commun.* **1995**, 1703.

(11) Mani, N. S.; Beall, L. S.; White, A. J. P.; Williams, D. J.; Barrett, A. G. M.; Hoffman, B. M. *J. Chem. Soc., Chem. Commun.* **1994**, 1943.

(12) Adams, K. R.; Bonnett, R.; Burke, P. J.; Salgado, A.; Valles, M. A. *J. Chem. Soc., Perkin Trans. 1* **1997**, 1769.

(13) Begland, R. W.; Hartter, D. R.; Jones, F. N.; Sam, D. J.; Sheppard, W. A.; Webster, O. W.; Weigert, F. J. *J. Org. Chem.* **1974**, *39*, 2341.

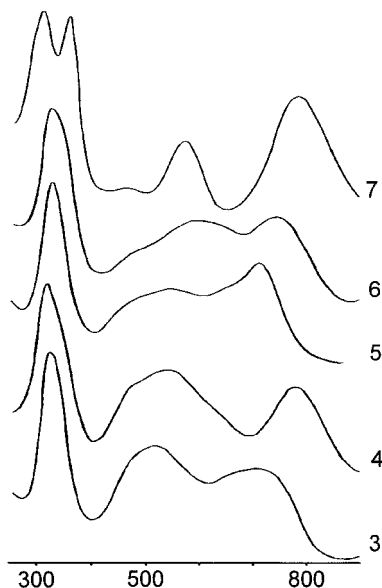


Figure 1. UV-vis spectra for porphyrazines **3**–**7** in CH_2Cl_2 .

in propanol provided **2** (MgODMAPz) in up to 48% yield, and traces of a less polar purple pigment (Scheme 1). Compound **2** showed an electronic absorption spectrum typical of porphyrazines, with the Q-band at 752 nm, an intense peak at 599 nm, and a band in the Soret region at 335 nm. We assigned the peak at 599 nm to the $n-\pi^*$ transition of the lone-pair electrons on the peripheral nitrogen atoms into a π^* ring orbital. A single resonance corresponding to *N*-methyl groups in the proton NMR spectrum, and further spectroscopic data, are in full agreement with the proposed structure. X-ray crystallographic determinations were carried out on related octaaminoporphyrazines.⁷ The spectroscopic signature of the less polar purple pigment was most curious. First, both the ^1H and ^{13}C NMR spectra showed that the compound lacked the expected D_{4h} symmetry of the MgODMAPz **2**. Both microanalysis and high-resolution mass ion measurement were consistent with loss of the magnesium(II) cation and a composition of $\text{C}_{32}\text{H}_{50}\text{N}_{16}\text{O}_2$. The UV-vis spectrum also showed a loss of symmetry with a concomitant red-shift of the Q-band from 752 to 788 nm (Figure 1). Recrystallization of the purple pigment from ethyl acetate and hexanes gave iridescent green crystals suitable for an X-ray crystallographic study.¹¹

This study unequivocally established the structure of the purple pigment as the seco-porphyrazine **4**. The structure is disordered (80:20) about a noncrystallographic inversion center in the middle of the "porphyrazine" ring; the major occupancy conformer is illustrated in Figure 2 and shows the two amido carbonyl groups to be *anti* and steeply inclined (ca. 58°) to the ring plane. The opening of one of the pyrrole rings produces a small C_2 distortion [about the $\text{N}(1)\cdots\text{N}(21)$ vector] of the "porphyrazine" core with $\text{N}(3)$ and $\text{N}(18)$ lying 0.17 and 0.14 Å above and below the inner N_4 plane, respectively (which is coplanar to within 0.03 Å). The molecules pack to form stepped polar stacks with a mean interplanar separation of 4.05 Å, the adjacent "porphyrazine" ring centroids being separated by 6.27 Å, Figure 3. The ^1H and ^{13}C NMR spectra for this substance showed five distinct *N*-methyl groups, six ring carbons, and an amide

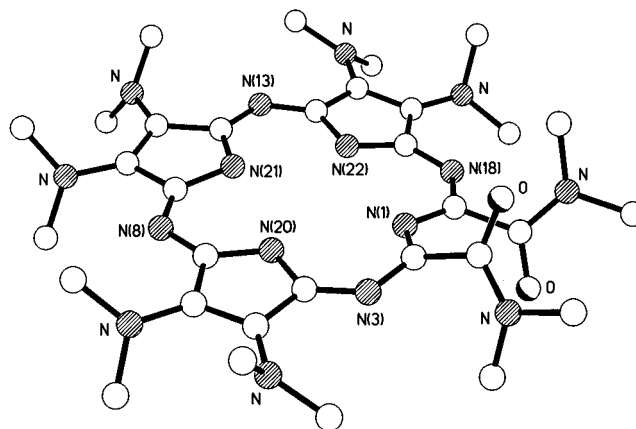


Figure 2. The molecular structure of **4**.

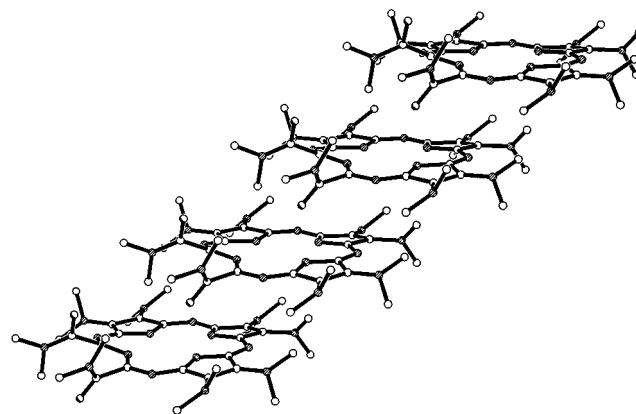
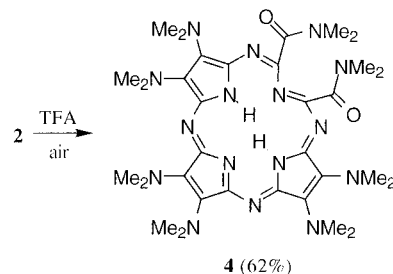


Figure 3. Part of one of the polar stacks present in the structure of **4**.

Scheme 2



carbonyl. These features are fully consistent with structure **4** and with slow rotation about the amide C–N bonds.

Demetalation of the magnesium complex **2** with trifluoroacetic acid under an inert atmosphere gave the expected free base porphyrazine **3**, but in only 21% yield. With glacial acetic acid, however, the desired product **3** was obtained in a much improved 69% yield (Scheme 1). The electronic absorption spectrum of H_2ODMAPz **3** is qualitatively the same as that of **2** (not shown), except that the Q-band and the $n-\pi^*$ transition are blue-shifted to 709 and 531 nm, respectively (Figure 1). In a control experiment, demetalation of the porphyrazine **2** using trifluoroacetic acid in the presence of air gave exclusively the previously observed pigment **4** (vide supra) (Scheme 2).

The annulene-type cyclic, conjugated, 18 π -electron system in **2**, in conjunction with the dimethylamino groups acting as strong electron donors, results in the ODMAPz macrocycle having two opposed, *quasi* isolated

(14) Linstead, R. P.; Whalley, M. *J. Chem. Soc.* **1952**, 4839.

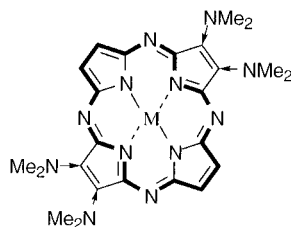


Figure 4.

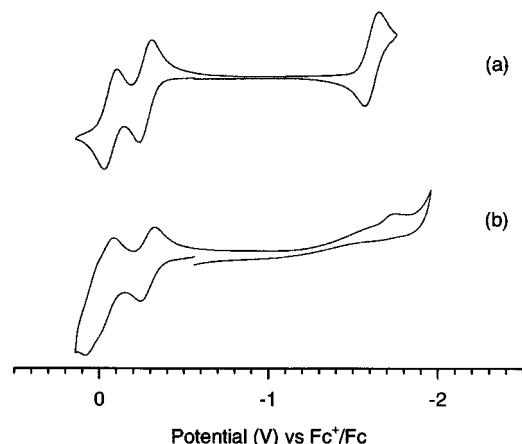
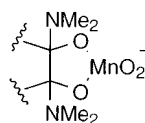
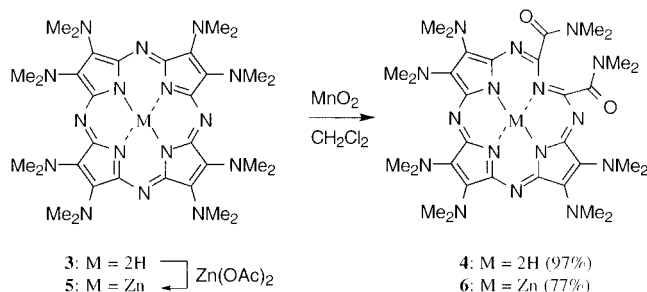
Figure 5. Cyclic voltammograms of (a) H₂ODMAPz **3** and (b) ZnODMAPz **5** (potential vs Fc⁺/Fc).

Figure 6.

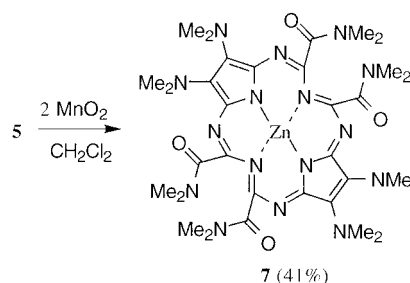
and very electron rich double bonds (Figure 4). We speculated that as a result of these combined properties, *seco*-porphyrazine **4** was formed via a formal 2 + 2 cycloaddition of singlet oxygen to one of the activated pyrrole rings, followed by cleavage (retro 2 + 2) of the dioxetane intermediate. We envisaged, therefore, that high-valent metal oxides should cause a similar type of oxidative ring scission, resulting in the formation of the same product. Furthermore, a controlled second pyrrole cleavage could give access to *trans*-diseco-porphyrazines. In fact, *seco*-porphyrazine **4** was obtained in high yield after a very dilute solution of H₂ODMAPz **3** was treated with 1 equiv of manganese dioxide at ambient temperature for 24 h. At higher concentrations, with an excess of manganese dioxide, or with the stronger oxidant potassium permanganate, however, only slow decomposition and no formation of any of the corresponding *seco*- or diseco-porphyrazine was observed. However, oxidation of the core metalated ODMAPz derivative **5**, for which the first reversible oxidation is centered at a value close to that of the free base **3** ([H₂Pz]⁺/[H₂Pz], $E^{1/2} = -269$ mV⁹ and [ZnPz]⁺/[ZnPz], $E^{1/2} = -280$ mV [vs Fc⁺/Fc]) (Figure 5), provided not only the monocleaved product but also the desired diseco-porphyrazine. ZnODMAPz **5** was prepared in high yield (82%) from reaction of H₂ODMAPz **3** with zinc(II) acetate. Subsequent oxidation of the zinc complex **5** to *seco*-porphyrazine **6** occurred readily with 1 equiv only of manganese dioxide in 4 h (Scheme 3).

Prolonged reaction times, or the use of an excess of the oxidant, resulted in reduced yields of **6**, along with some

Scheme 3



Scheme 4



of the expected second pyrrole cleavage and decomposition. If porphyrazine **5** was treated with 2 equiv of manganese dioxide for 24 h, the rather unstable product of overoxidation, diseco-porphyrazine **7**, could be isolated in up to 41% yield (Scheme 4). By analogy with the proposed oxidation via singlet oxygen (vide supra), the manganese-mediated ring scission is likely to involve a cyclic intermediate as exemplified in Figure 6.

While the electronic absorption spectra of porphyrazines **5** and **6** resembled those described earlier, the spectral changes for diseco-porphyrazine **7** indicated a low degree of symmetry ($D_{4h} \rightarrow D_{2h}$). We tentatively suggest that the peaks centered at 789 and 579 nm correspond to the red-shifted split Q-band, and that the $n-\pi^*$ peak was reduced to a small shoulder centered at 470 nm. In accordance with Gouterman's four-orbital model,¹⁵ the Soret region was also split into two absorptions which appear at 363 and 314 nm (Figure 1).

While the free base *seco*-porphyrazine **4** gave a sharp, well-resolved ¹H NMR spectrum in CDCl₃, the ¹H NMR spectra of zinc-*seco*- and zinc-diseco-porphyrazines **6** and **7** displayed very broad signals. This broadening could be overcome by adding pyridine-*d*₅ to the samples or by recording the NMR spectra in this solvent. This effect can be rationalized by assuming an interaction between the zinc center of one macrocycle with the Lewis basic amide oxygen of a second *seco*-porphyrazine resulting in the formation of dimers (vide infra), which could be disassembled in solution by the presence of the coordinating solvent pyridine. While the ¹H and ¹³C NMR spectra of compounds **4** and **6** were qualitatively the same, the ¹H and ¹³C NMR spectra of diseco-porphyrazine **7** showed three distinct *N*-methyl resonances and a single amide carbonyl. These features combined with high-resolution mass ion measurement are in agreement with structure **7**, in which the two cleaved pyrrole rings are in a *trans*-disposition.

This convenient method was further extended to unsymmetrical porphyrazines. Thus, reaction of the free

(15) Gouterman, M. In *The Porphyrins*, Dolphin, D., Ed.; Academic Press, Inc.: New York, 1978.

(16) Lange, S. J.; Stern, C. L.; Barrett, A. G. M.; Hoffman, B. M. Manuscript in preparation.

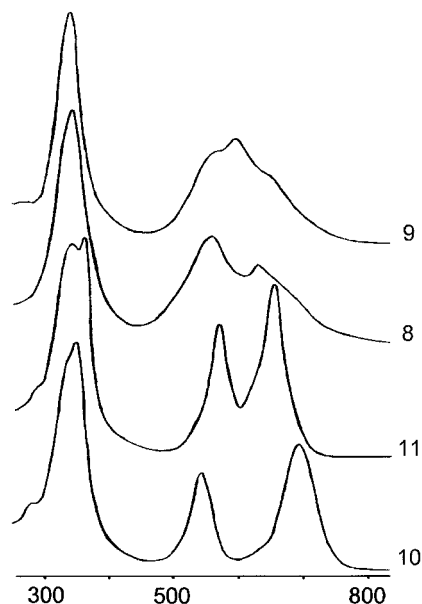
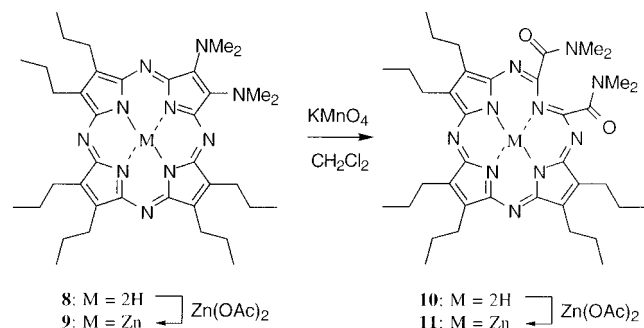


Figure 7. UV-vis spectra for porphyrazines **8–11** in $\text{CH}_2\text{-Cl}_2$.

Scheme 5



base porphyrazine **8**¹⁶ with zinc(II) acetate resulted in selective metalation within the macrocyclic cavity to provide the corresponding zinc complex **9** in high yield. Both **8** and **9** were unreactive toward oxidation by manganese dioxide. However, reaction of compounds **8** and **9** with potassium permanganate gave the expected seco-porphyrazines **10** and **11**, respectively, in 93 and 96% yield (Scheme 5). In both cases, under optimized conditions, a 10-fold excess of the oxidant effected complete reaction in less than 3 h. Alternatively, zinc-seco-porphyrazine **11**, was obtained in high yield (97%) from the reaction of seco-porphyrazine **10** with zinc(II) acetate. Reversing the order of reactions (oxidation and then metalation instead of metalation followed by oxidation), as in the above example, could prove useful for the synthesis of otherwise inaccessible core metalated seco-porphyrazines. In contrast to the electronic absorption spectra of the nonoxidized materials **8** and **9**, the electronic absorption spectra of seco-porphyrazines **10** and **11** display a split red-shifted Q-band at 693 and 543 and at 649 and 565 nm, respectively. In addition to the red-shifted Q-band, the optical spectrum of the zinc-seco-porphyrazine **11** shows also a split band in the Soret region at 356 and 339 nm (Figure 7). The same solvent dependency phenomenon previously noticed in the ¹H NMR spectra of **6** and **7** was also observed in the ¹H NMR spectra of seco-porphyrazines **10** and **11** (vide supra). Thus, while the free base seco-porphyrazine **10** gave again a well resolved ¹H NMR spectrum in CDCl_3 , the

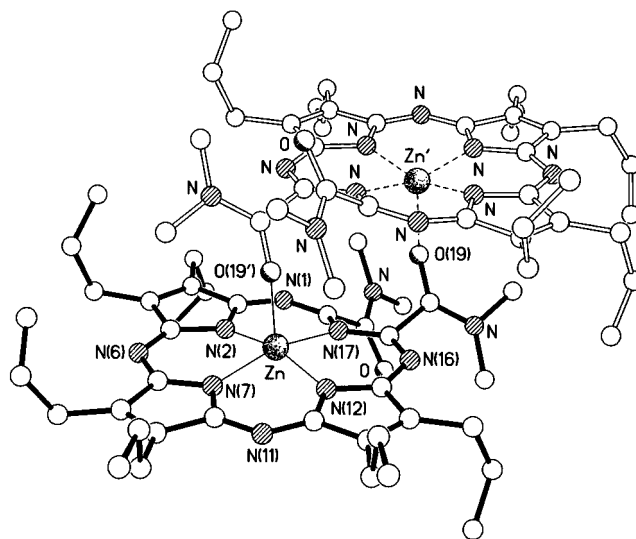


Figure 8. The molecular structure of **11**. Selected bond lengths (Å) and angles (deg): Zn–N(2) 1.965(3), Zn–N(7) 2.025(3), Zn–N(12) 1.962(3), Zn–N(17) 2.138(3), Zn–O(19') 2.123(3), N(12)–Zn–N(2) 162.0(1), N(12)–Zn–N(7) 87.6(1), N(2)–Zn–N(7) 87.5(1), N(12)–Zn–O(19') 99.8(1), N(2)–Zn–O(19') 98.0(1), N(7)–Zn–O(19') 95.7(1), N(12)–Zn–N(17) 90.0(1), N(2)–Zn–N(17) 89.4(1), N(7)–Zn–N(17) 162.3(1), O(19')–Zn–N(17) 102.0(1).

¹H NMR spectrum of the zinc-seco-porphyrazine **11** had to be recorded in pyridine-*d*₅ in order to avoid broadening. Furthermore, a solvent dependent stability of the zinc-porphyrazines **5**, **6**, and **9** in solution was noticed; while these macrocycles seem to be indefinitely stable in coordinating solvents such as pyridine or DMF, oxidation to the corresponding seco-porphyrazines **6**, **7**, and **11** occurred when solutions of the zinc complexes **5**, **6**, and **9** were left standing for prolonged times in chlorinated solvents (CH_2Cl_2 or CHCl_3).

Slow evaporation of a solution of compound **11** in $\text{CH}_2\text{-Cl}_2$ /hexanes (1:1) gave iridescent purple crystals suitable for X-ray crystallography. The structural analysis reveals the formation of C_i symmetric dimer pairs in the solid state wherein one of the amido oxygen atoms of one molecule occupies the apical site of the square pyramidal coordination of the zinc(II) center of the next and *vice versa* (Figure 8). The zinc atom lies 0.31 Å out of the basal plane (which is coplanar to within 0.007 Å) in the direction of the apical oxygen atom. There is a noticeable asymmetry in the Zn–N bond distances which range between 1.962(3) and 2.138(3) Å; the shorter distances are to the *trans*-pyrrole nitrogen atoms and are closer to the values observed for square planar zinc(II) coordination in such systems,¹⁷ cf. square pyramidal.^{18–20} The Zn–O distance of 2.123(3) Å is unexceptional and typical for a covalently bonded oxygen atom.

As in the structure of **4** the amido carbonyl groups are *anti* and similarly inclined to the ring plane (ca. 53°, cf. 58° in **4**). The opening of one of the pyrrole rings again produces a small C_2 distortion of the "porphyrazine" core about the N(7)···N(17) vector, N(1) and N(16) lying 0.18 and 0.10 Å below and above (in the direction of the

(17) Scheidt, W. R.; Dow, W. *J. Am. Chem. Soc.* **1977**, *99*, 1101.

(18) Kobayashi, T.; Ashida, T.; Uyeda, N.; Suito, E.; Kakudo, M. *Bull. Chem. Soc., Jpn.* **1971**, *44*, 2095.

(19) Assmann, B.; Sievertsen, S.; Homborg, H. *Acta Crystallogr. C* **1996**, *52*, 876.

(20) Mossoyan-Deneux, M.; Benlian, D.; Pierrot, M.; Fournel, A.; Sobrier, J. P. *Inorg. Chem.* **1985**, *24*, 1878.

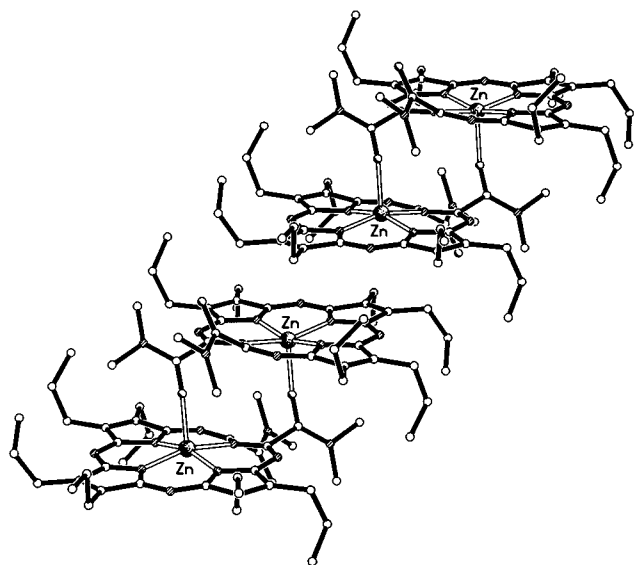


Figure 9. Part of one of the stacks of back-to-back dimer pairs present in the structure of **11**.

coordinated zinc atom) the inner N_4 plane, respectively. The mean interplanar separation of the "porphyrazine" cores within the dimer is 3.91 Å, the nonbonded $Zn \cdots Zn$ distance being 5.54 Å, and the separation of the centroids of the two inner N_4 rings being 5.91 Å, cf. 6.27 Å in **4**.

The dimer pairs form stepped stacks in the crystallographic a direction with a mean interplanar separation of back-to-back N_8 rings in adjacent dimers of 3.41 Å—a separation significantly shorter than that *within* the dimer pairs—the associated centroid \cdots centroid and $Zn \cdots Zn$ distances being 5.61 and 6.00 Å, respectively (Figure 9). It is interesting to note that even though the nature of the peripheral substituents on **4** and **11** are different, the complexation of zinc has little effect on the supramolecular stacked arrangement of the "porphyrazine" components.

Conclusions

We have successfully carried out the synthesis and structural characterization of a new family of tetraaza-macrocycles, the seco-porphyrazines. The different molecular symmetries of the porphyrazine precursors and the cleaved products have a profound effect on the electronic structure of each macrocycle. Furthermore, zinc-seco-porphyrazines show an interesting novel feature, namely the manner in which the macrocyclic units are held together through coordination of the zinc(II) cation in one molecule to one of the amide oxygen atoms in the other and *vice versa*. Clearly the synthetic strategy is flexible and should be suitable for the preparation of a wide number of seco- and diseco-porphyrazines whose properties and metal ion complexation capabilities will be the subject of future reports.

Experimental Section

General Procedures. All reactions were conducted in oven- or flame-dried glassware. Reaction temperatures reported refer to external bath temperatures. Hexanes refers to the petroleum fraction bp 40–60 °C. Solvents used for reactions were distilled prior to use: THF (from sodium benzophenone ketyl); dichloromethane (from CaH_2); DMF [predried over BaO, distilled from alumina (activity I)]; propanol and butanol (from Mg). All other reagents were used

as commercially supplied. TLC was carried out on E. Merck precoated silica gel 60 F₂₅₄ plates. Plates were visualized using UV radiation (254 nm). Chromatography refers to flash chromatography on E. Merck silica gel 60, 40–60 μ m. Size exclusion chromatography was performed on Sephadex LH-20. Cyclic voltametric measurements were carried out with a Cypress Systems 1087 computer-controlled potentiostat.

[2,3,7,8,12,13,17,18-Octakis(dimethylamino)porphyrazinato]magnesium(II) (2). A mixture of propanol (200 mL), Mg (2.36 g), and I_2 (3 small crystals) was heated to reflux for 12 h under N_2 . The suspension was cooled and a solution of 1,2-bis(dimethylamino)maleonitrile (**1**)¹³ (4.0 g, 24.3 mmol) in propanol (15 mL) was added and the reaction mixture further heated at reflux for 36 h. The deep blue suspension was allowed to cool and filtered (Celite), and the solids were washed with Et_2O . Rotary evaporation, chromatography ($Et_2O:CHCl_3:MeOH$ 9:9:2), and gel filtration ($CHCl_3$) provided porphyrazine **2** (2 g, 48%) as a black crystalline solid with purple reflections: mp > 350 °C; R_f 0.13 ($EtOAc:hexanes$ 1.5:1); IR (CH_2Cl_2) 2920, 2865, 2776, 1573, 1365, 1065 cm^{-1} ; UV-vis λ_{max} (log ϵ) = 335 (4.81), 599 (4.27), 752 (4.33), CH_2Cl_2 ; 1H NMR (300 MHz, $CDCl_3$) δ 3.38 (s); HRMS (EI) calcd for $C_{32}H_{48}MgN_{16}$: $[M]^+$, 680.4098, found: $[M]^+$, 680.4091. Anal. Calcd for $C_{32}H_{48}MgN_{16}$: C, 56.41; H, 7.11; N, 32.91. Found: C, 56.19; H, 7.35; N, 32.15.

2,3,7,8,12,13,17,18-Octakis(dimethylamino)porphyrazine (3). Acetic acid (25 mL) was added to porphyrazine **2** (300 mg, 0.44 mmol) and the mixture stirred at 20 °C for 30 min under N_2 . The solution was poured onto ice and water (250 mL) and the resulting suspension brought to pH 7.0–7.5 with 1M NaOH. The solid was collected via vacuum filtration and washed with water. Column chromatography (hexanes: $EtOAc$ 5:1) and gel filtration ($CHCl_3$) provided porphyrazine **3** (200 mg, 69%) as a dark purple solid: mp > 350 °C; R_f 0.70 ($EtOAc:hexanes$ 1.5:1); IR (Nujol) 3400, 3280, 2910, 2790, 1588, 1567, 1376, 1196, 1071 cm^{-1} ; UV-vis λ_{max} (log ϵ) = 334 (4.57), 531 (4.29), 709 (4.16), CH_2Cl_2 ; 1H NMR (300 MHz, $CDCl_3$) δ 3.8 (s, 48H), -0.93 (s, 2H); ^{13}C NMR (75 MHz, $CDCl_3$) δ 45.1, 137.8, 148.7; HRMS (EI) calcd for $C_{32}H_{50}N_{16}$: $[M]^+$, 658.4404, found: $[M]^+$, 658.4437.

2,3,7,8,12,13,17,18-Octakis(dimethylamino)-2-secoporphyrazine-2,3-dione (4). (1) TFA (5 mL) was added to porphyrazine **2** (100 mg, 0.102 mmol) and the resulting solution stirred at 20 °C under an atmosphere of air for 30 min. The solution was poured onto ice and water (100 mL) and the resulting suspension brought to pH 7.0–7.5 with 1M NaOH. The solid was collected via vacuum filtration and washed with water. Column chromatography (hexane: $EtOAc$ 9:1) gave seco-porphyrazine **4** (44 mg, 62%) as a dark purple solid: mp 280–285 °C; R_f 0.10 (hexane: $EtOAc$ 2.3:1); IR ($CHCl_3$) 3053, 2927, 1639, 1577, 1519, 1383, 1265, 1042, 1006, 729, 709 cm^{-1} ; UV-vis λ_{max} (log ϵ) = 323 (4.76), 542 (4.53), 788 (4.46), CH_2Cl_2 ; 1H NMR (270 MHz, $CDCl_3$) δ 0.05 (s, 2H), 3.34 (s, 6H), 3.44 (s, 12H), 3.57 (s, 12H), 3.79 (s, 6H), 3.86 (s, 12H); ^{13}C NMR (75 MHz, $CDCl_3$) δ 35.3, 40.2, 43.9, 45.2, 45.3, 129.7, 136.4, 139.3, 141.0, 153.4, 154.7, 169.8; MS (FAB) m/z 690, 618; HRMS (FAB) calcd for $C_{32}H_{50}N_{16}O_2$: $[M]^+$, 690.4303, found: $[M]^+$, 690.4318. Anal. Calcd for $C_{32}H_{50}N_{16}O_2$: C, 55.62; H, 7.30; N, 32.45. Found: C, 55.84; H, 7.05; N, 32.17.

(2) To a solution of porphyrazine **3** (5 mg, 0.008 mmol) in CH_2Cl_2 (50 mL) was added MnO_2 (0.7 mg, 0.008 mmol) and the mixture stirred at 20 °C for 24 h. The resulting purple solution was filtered (Celite), and the solids were washed with CH_2Cl_2 . Rotary evaporation and chromatography (10% $EtOAc$ in hexane then $EtOAc$) gave seco-porphyrazine **4** (5.1 mg, 97%) as a dark purple solid. Crystal data for **4**: $C_{32}H_{50}N_{16}O_2$, $M = 690.9$, triclinic, space group $\bar{P}1$ (no. 1), $a = 6.270(4)$, $b = 11.210(7)$, $c = 14.108(9)$ Å, $\alpha = 103.90(2)$, $\beta = 102.77(2)$, $\gamma = 101.46(2)^\circ$, $V = 905(1)$ Å³, $Z = 1$, $D_c = 1.27$ g cm^{-3} , $\mu(Cu K\alpha) = 7.0$ cm^{-1} , $F(000) = 370$. A dark green iridescent platy needle of dimensions $0.97 \times 0.37 \times 0.12$ mm was used. 2967 Independent data were measured on a Siemens P4/PC diffractometer at 293 K with Cu $K\alpha$ radiation (graphite monochromator) using ω -scans. The structure was solved by direct methods, and the non-hydrogen atoms were refined anisotropically using full matrix least-squares based on F to give $R =$

0.046, $R_w = 0.053$ for 2785 independent observed reflections [$|F_o| > 4\sigma(|F_o|)$, $2\theta \leq 130^\circ$] and 545 parameters. The structure is partially disordered with ca. 20% of the molecules inverted about the center of the porphyrazine ring.

[2,3,7,8,12,13,17,18-Octakis(dimethylamino)porphyrazinato]zinc(II) (5). A solution of porphyrazine **3** (100 mg, 0.15 mmol) in dry DMF (10 mL) was heated at 50 °C with anhydrous Zn(OAc)₂ (27.8 mg, 0.15 mmol) for 6 h under N₂. The reaction mixture was allowed to cool and filtered (Celite), and the solids were washed with CH₂Cl₂. Rotary evaporation and chromatography (hexane:EtOAc 9:1) gave Zn-ODMAPz **5** (90 mg, 82%) as a dark blue crystalline solid: mp > 350 °C; R_f 0.35 (EtOAc:hexane 1.5:1); IR (CH₂Cl₂) 2928, 1574, 1491, 1446, 1381, 1312, 1266, 1212, 1141, 1090 cm⁻¹; UV-vis λ_{max} (log ϵ) = 335 (4.69), 546 (4.32), 718 (4.46), CH₂Cl₂; ¹H NMR (300 MHz, CDCl₃) δ 3.78 (s); ¹³C NMR (75 MHz, CDCl₃) δ 44.9, 138.8, 152.2; MS (FAB) m/z 720; HRMS (FAB) calcd for C₃₂H₄₉N₁₆Zn: [M + H]⁺, 721.3618, found: [M + H]⁺, 721.3676. Anal. Calcd for C₃₂H₄₈N₁₆Zn: C, 53.22; H, 6.70. Found: C, 53.20; H, 6.69.

[2,3,7,8,12,13,17,18-Octakis(dimethylamino)-2-seco-2,3-dioxoporphyrazinato]zinc(II) (6). To a solution of Zn-ODMAPz **5** (5 mg, 0.007 mmol) in CH₂Cl₂ (3 mL) was added MnO₂ (0.61 mg, 0.007 mmol) and the mixture stirred at 20 °C for 4 h. The resulting blue solution was filtered (Celite), and the solids were washed with CH₂Cl₂. Rotary evaporation and chromatography (10% EtOAc in hexane then EtOAc) gave zinc-seco-porphyrazine **6** (4 mg, 77%) as a dark blue solid: mp > 350 °C; R_f 0.13 (EtOAc:hexane 1.5:1); IR (CH₂Cl₂) 3060, 2927, 1721, 1633, 1578, 1493, 1383, 1131, 1078, 879, 806 cm⁻¹; UV-vis λ_{max} (log ϵ) = 334 (4.80), 594 (4.46), 747 (4.46), CH₂Cl₂; ¹H NMR (300 MHz, pyridine-*d*₅) δ 3.18 (s, 6H), 3.24 (s, 12H), 3.54 (s, 12H), 3.56 (s, 12H), 3.74 (s, 6H); ¹³C NMR (75 MHz, pyridine-*d*₅) δ 34.6, 39.5, 43.9, 44.7, 44.9, 132.9, 138.6, 141.8, 147.9, 152.3, 154.6, 169.5; MS (FAB) m/z 753 [M - H]⁺, 680.

[2,3,7,8,12,13,17,18-Octakis(dimethylamino)-2,12-diseco-2,3,12,13-tetraoxoporphyrazinato]zinc(II) (7). The same reaction as above, but with 2 equiv of MnO₂ (4.9 mg, 0.056 mmol) and 24 h, gave the title compound after chromatography (EtOAc and then pyridine) and gel filtration (CHCl₃) as a dark purple solid (9 mg, 41%): mp > 350 °C; R_f 0.19 (EtOAc); IR (CH₂Cl₂) 2927, 2855, 1640, 1600, 1499, 1380, 1253, 1130, 1055 cm⁻¹; UV-vis λ_{max} (log ϵ) = 314 (4.40), 363 (4.39), 470 (3.80), 579 (4.05), 789 (4.20), CH₂Cl₂; ¹H NMR (300 MHz, pyridine-*d*₅) δ 3.39 (s, 12H), 3.5 (s, 24H), 3.95 (s, 12H); ¹³C NMR (75 MHz, pyridine-*d*₅) δ 36.1, 40.9, 45.6, 170.9; MS (FAB) m/z 785, 680; HRMS (FAB) calcd for C₃₂H₄₉N₁₆O₄Zn: [M + H]⁺, 785.3414, found: [M + H]⁺, 785.3461.

[2,3-Bis(dimethylamino)-7,8,12,13,17,18-hexapropylporphyrazinato]zinc(II) (9). A solution of porphyrazine **8**¹⁶ (30 mg, 0.045 mmol) in dry DMF (10 mL) was heated at 70 °C with anhydrous Zn(OAc)₂ (8.4 mg, 0.046 mmol) for 16 h under N₂. The reaction mixture was allowed to cool and filtered (Celite), and the solids were washed with CH₂Cl₂. Rotary evaporation and chromatography (hexane:EtOAc 9:1) gave zinc-porphyrazine **9** (29 mg, 89%) as a dark blue solid: mp 220–240 °C; R_f 0.71 (hexane:EtOAc 2.3:1); IR (CH₂Cl₂) 2956, 2928, 2862, 1725, 1604, 1580, 1463, 1370, 1293, 1145, 1092, 1023, 954 cm⁻¹; UV-vis λ_{max} (log ϵ) = 341 (4.82), 597 (4.48), CH₂Cl₂; ¹H NMR (300 MHz, CDCl₃) δ 1.22–1.54 (m, 18H), 2.18–2.28 (m, 12H), 3.68–3.73 (m, 12H), 3.89 (s, 12H); ¹³C NMR (75 MHz, pyridine-*d*₅) δ 14.8, 25.8, 28.5, 44.3, 137.7, 142.7, 143.6, 155.9, 157.0, 157.6, 158.2; MS (FAB) m/z 715; HRMS (FAB) calcd for C₃₈H₅₄N₁₀Zn: [M + H]⁺, 715.3903, found: [M + H]⁺, 715.3906.

2,3-Bis(dimethylamino)-7,8,12,13,17,18-hexapropyl-2-secoporphyrazine-2,3-dione (10). To a solution of porphyrazine **8**¹⁶ (5 mg, 0.0075 mmol) in CH₂Cl₂ (3 mL) was added KMnO₄ (12 mg, 0.075 mmol) and the mixture stirred at 20 °C for 3 h. The resulting purple solution was filtered (Celite), and the solids were washed with CH₂Cl₂. Rotary evaporation and chromatography (10–20% EtOAc in hexanes) gave seco-porphyrazine **10** (4.9 mg, 93%) as a dark purple solid: mp 160–200 °C; R_f 0.25 (hexane:EtOAc 2.3:1); IR (CH₂Cl₂) 2962,

2932, 2872, 1731, 1643, 1496, 1463, 1402, 1121, 981, 936 cm⁻¹; UV-vis λ_{max} (log ϵ) = 348 (4.75), 543 (4.39), 693 (4.49), CH₂Cl₂; ¹H NMR (300 MHz, CDCl₃) δ -1.29 (s, 2H), 1.17–1.43 (m, 18H), 2.06–2.35 (m, 12H), 3.44 (s, 6H), 3.67 (t, $J = 7.52$ Hz, 4H), 3.78 (t, $J = 7.74$ Hz, 4H), 3.85 (t, $J = 7.58$ Hz, 4H), 3.96 (s, 6H); ¹³C NMR (75 MHz, CDCl₃) δ 14.7, 14.8, 25.3, 25.4, 25.6, 27.7, 28.1, 35.3, 40.0, 139.7, 142.0, 142.6, 144.0, 144.3, 154.1, 161.4, 168.9; MS (FAB) m/z 683 [M - H]⁺, 612; HRMS (FAB) calcd for C₃₅H₅₀N₉O: [M - CONMe₂]⁺, 612.4138, found: [M - CONMe₂]⁺, 612.4155.

[2,3-Bis(dimethylamino)-7,8,12,13,17,18-hexapropyl-2-seco-2,3-dioxoporphyrazinato]zinc(II) (11). (1) Treatment of porphyrazine **9** (5 mg, 0.007 mmol) under the same reaction conditions as above gave zinc-seco-porphyrazine **11** (5 mg, 96%) as a dark blue solid: mp 340 °C; R_f 0.19 (hexane:EtOAc 2.3:1); IR (CH₂Cl₂) 2960, 2931, 2871, 1725, 1634, 1605, 1494, 1463, 1402, 1138, 1009, 957 cm⁻¹; UV-vis λ_{max} (log ϵ) = 339 (4.67), 356 (4.69), 565 (4.47), 649 (4.59), CH₂Cl₂; ¹H NMR (300 MHz, pyridine-*d*₅) δ 1.17 (t, $J = 7.28$ Hz, 6H), 1.27–1.40 (m, 12H), 2.10–2.24 (m, 4H), 2.33–2.53 (m, 8H), 3.46 (s, 6H), 3.70 (t, $J = 7.44$ Hz, 4H), 3.87 (t, $J = 7.44$ Hz, 4H), 3.95 (t, $J = 7.43$ Hz, 4H), 4.10 (s, 6H); ¹³C NMR (75 MHz, pyridine-*d*₅) δ 16.1, 16.3, 27.1, 27.3, 29.3, 29.7, 29.8, 36.4, 41.1, 142.6, 143.7, 146.1, 155.8, 156.0, 157.4, 159.5, 170.9; MS (FAB) m/z 747 [M - H]⁺, 674; HRMS (FAB) calcd for C₃₅H₄₈N₉OZn: [M - CONMe₂]⁺, 674.3273, found: [M - CONMe₂]⁺, 674.3264. Anal. Calcd for C₃₈H₅₄N₁₀O₂Zn: C, 60.99; H, 7.27; N, 18.72. Found: C, 60.99; H, 7.11; N, 18.39.

(2) A solution of seco-porphyrazine **10** (5 mg, 0.0073 mmol) in dry DMF (2 mL) was heated at 50 °C with anhydrous Zn(OAc)₂ (1.3 mg, 0.0073 mmol) for 2 h under N₂. The reaction mixture was allowed to cool and filtered (Celite), and the solids were washed with CH₂Cl₂. Rotary evaporation and chromatography (10–20% EtOAc in hexanes) gave zinc-seco-porphyrazine **11** (5.3 mg, 97%) as a dark blue solid. Crystal data for **11**: C₇₆H₁₀₈N₂₀O₄Zn₂, $M = 1496.6$, triclinic, space group $P\bar{1}$ (no. 2), $a = 11.516(1)$, $b = 12.446(1)$, $c = 15.125(1)$ Å, $\alpha = 113.47(1)$, $\beta = 98.28(1)$, $\gamma = 96.10(1)^\circ$, $V = 1935.6(2)$ Å³, $Z = 1$ (the molecule has crystallographic C_i symmetry), $D_c = 1.28$ g cm⁻³, $\mu(\text{Cu K}\alpha) = 12.5$ cm⁻¹, $F(000) = 796$. A purple iridescent platy needle of dimensions 0.40 × 0.13 × 0.07 mm was used. 5519 Independent data were measured on a Siemens P4/RA diffractometer at 203 K with Cu K α radiation (graphite monochromator) using ω -scans. The structure was solved by direct methods and all the non-hydrogen atoms were refined anisotropically using full matrix least-squares based on F^2 using absorption corrected data (based on ψ -scans; max. and min transmission factors 0.86 and 0.77 respectively) to give $R_1 = 0.061$, $wR_2 = 0.156$ for 4580 independent observed reflections [$|F_o| > 4\sigma(|F_o|)$, $2\theta \leq 120^\circ$] and 460 parameters. The crystallographic data (excluding structure factors) for **11** have been deposited with the Cambridge Crystallographic Data Centre (the corresponding data for **4** was deposited with the original communication¹¹). Copies of the data can be obtained free of charge on application to The Director, CCDC, 12 Union Road, Cambridge, CB12 1EZ, UK (Fax: Int. code +(1223)336-033; e-mail: teched@chemcrs.cam.ac.uk).

Acknowledgment. We thank Glaxo Group Research Ltd. for the generous endowment (A.G.M.B.), the Wolfson Foundation for establishing the Wolfson Centre for Organic Chemistry in Medical Science at Imperial College, the Engineering and Physical Sciences Research Council, the National Science Foundation, and NATO for generous support of our studies.

Supporting Information Available: Copies of ¹H and ¹³C NMR spectra of **3**, **5**, **6**, **7**, **9**, and **10** and X-ray data of **11** (20 pages). This material is contained in libraries on microfiche, immediately follows this article in the microfilm version of the journal, and can be ordered from the ACS; see any current masthead for ordering information.

JO971599X